QCD confinement and chiral crossovers, two critical points?

Pedro Bicudo[*][†]

CFTP, Dep. Física, Instituto Superior Técnico,
Av. Rovisco Pais, 1049-001 Lisboa, Portugal
E-mail: bicudo@ist.utl.pt

We study the QCD phase diagram, in particular we study the critical points of the two main QCD phase transitions, confinement and chiral symmetry breaking. Confinement drives chiral symmetry breaking, and, due to the finite quark mass, at small density both transitions are a crossover, while they are a first or second order phase transition in large density. We study the QCD phase diagram with a quark potential model including both confinement and chiral symmetry. We present the confinement of quark fields into a flux tube, obtained in SU(3) quenched lattice QCD, to illustrate the importance of the confining quark-antiquark potential. Our finite temperature confining potential is extracted from the Lattice QCD data of the Bielefeld group. Our formalism, the Coulomb gauge hamiltonian of QCD, is presently the only one able to microscopically include both a quark-antiquark confining potential and a vacuum condensate of quark-antiquark pairs. This model is able to address all the excited hadrons, and chiral symmetry breaking, at the same token. Our order parameters are the Polyakov loop and the quark mass gap. We address how the quark masses affect the critical point location in the phase diagram.

[*]Speaker.

[†]Presented at Many Faces of QCD, 2010, Ghent; work partly done with Marco Cardoso and Nuno Cardoso.
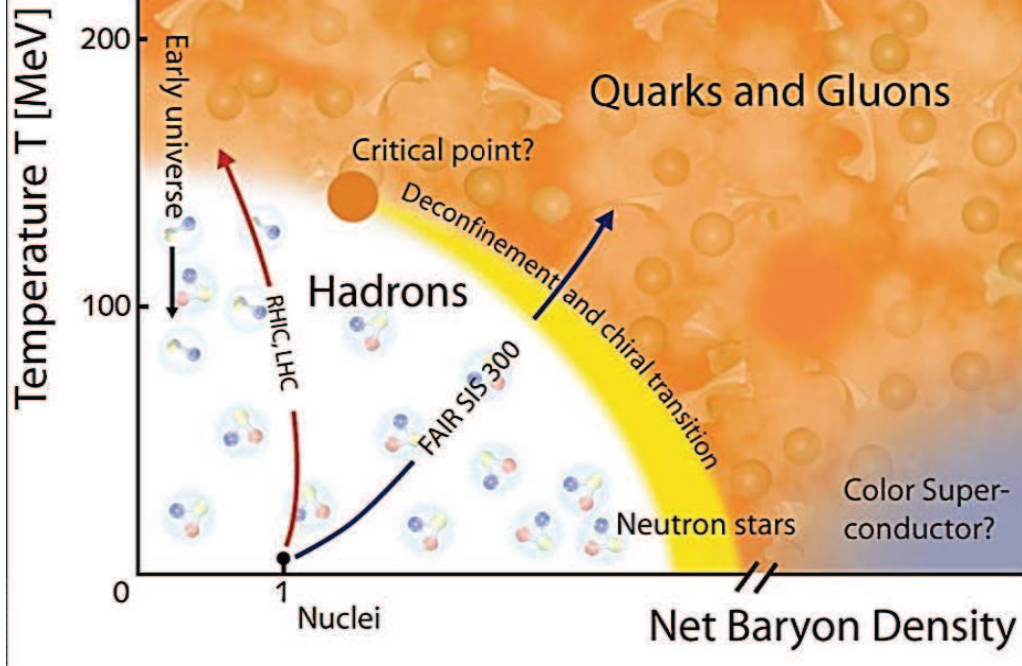
Figure 1: A sketch of the QCD Phase Diagram, according to the collaboration CBM at FAIR [1], it is usually assumed that the critical point for deconfinement coincides with the critical point for chiral symmetry restoration.

1. Introduction

Our main motivation is to contribute to understand the QCD phase diagram [1], for finite T and μ, to be studied at LHC, RHIC and FAIR, and sketched in Fig 1. Moreover, our formalism, in the Coulomb gauge hamiltonian formalism of QCD, is presently the only one able to microscopically include both a quark-antiquark confining potential and a vacuum condensate of quark-antiquark pairs. This model is able to address excited hadrons as in Fig. 2, and chiral symmetry at the same token, and we recently suggested that the infrared enhancement of the quark mass can be observed in the excited baryon spectrum at CBELSA and at JLAB [2, 3]. Thus the present work, not only addresses the QCD phase diagram, but it also constitutes the first step to allow us in the future to extend the computation of nay hadron spetrum, say the Fig. 1 (left) computed in reference [2], to finite T .

Here we address the finite temperature string tension, the quark mass gap for a finite current quark mass and temperature, and the deconfinement and chiral restoration crossovers. We conclude on the separation of the critical point for chiral symmetry restoration from the critical point for deconfinement.

2. Fits for the finite T string tension from the Lattice QCD energy F_1

At vanishing temperature $T = 0$, the confinement, due to the formation of chromo electric and chromo magnetic flux tubes as shown in Figs. 3 and 4, can be modelled by a string tension,
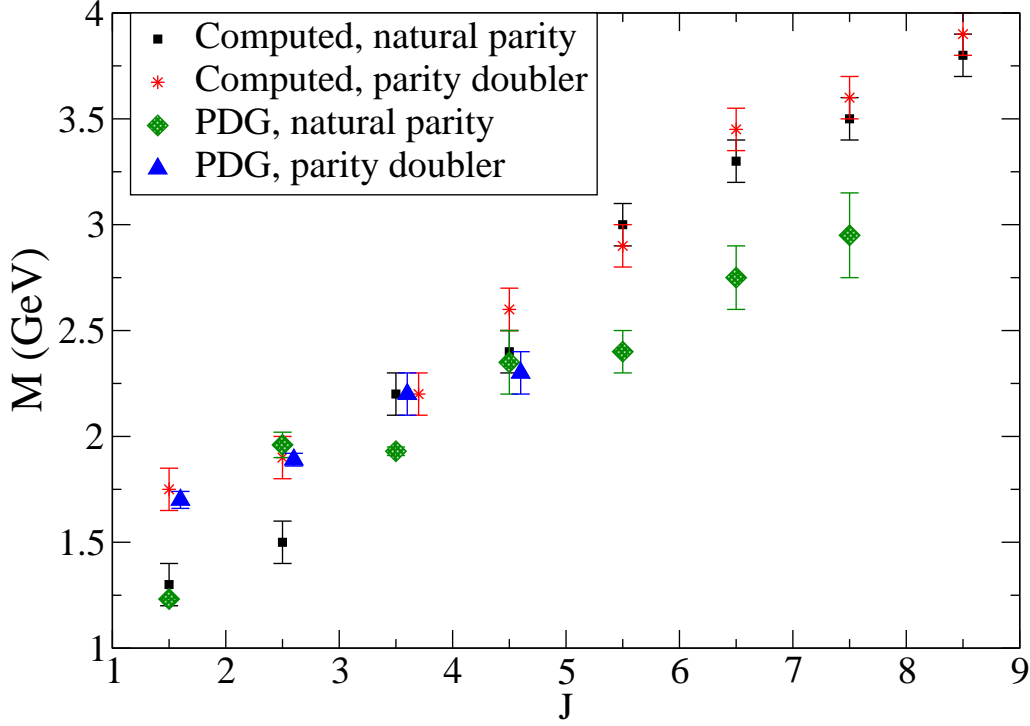
Figure 2: First calculation of excited baryons with a chiral invariant quark model.

dominant at moderate distances,

$$V(r) \simeq \frac{\pi}{12r} + V_0 + \sigma r \,. \tag{2.1}$$

At short distances we have the Luscher or Nambu-Gotto Coulomb due to the string vibration + the OGE coulomb, however the Coulomb is not important for chiral symmetry breaking. At finite temperature the string tension $\sigma(T)$ should also dominate chiral symmetry breaking, and thus one of our crucial steps here is the fit of the string tension $\sigma(T)$ from the Lattice QCD data of the Bielefeld Lattice QCD group, [4, 5, 6, 7, 8].

The Polyakov loop is a gluonic path, closed in the imaginary time t_4 (proportional to the inverse temperature T^{-1}) direction in QCD discretized in a periodic boundary euclidian Lattice. It measures the free energy F of one or more static quarks,

$$P(0) = Ne^{-F_q/T} \,, \;\; P^a(0)\bar{P}^{\bar{a}}(r) = Ne^{-F_{q\bar{q}}(r)/T} \,. \tag{2.2}$$

If we consider a single solitary quark in the universe, in the confining phase, his string will travel as far as needed to connect the quark to an antiquark, resulting in an infinite energy F. Thus the 1 quark Polyakov loop P is a frequently used order parameter for deconfinement. With the string tension $\sigma(T)$ extracted from the $q\bar{q}$ pair of Polyakov loops we can also estimate the 1 quark Polyakov loop $P(0)$. At finite T, we use as thermodynamic potentials the free energy F_1 and the internal energy U_1, computed in Lattice QCD with the Polyakov loop [4, 5, 6, 7, 8], and illustrated in Fig. 5. They are related to the static potential $V(r) = -fdr$ with $F1(r) = -fdr - SdT$ adequate for isothermic
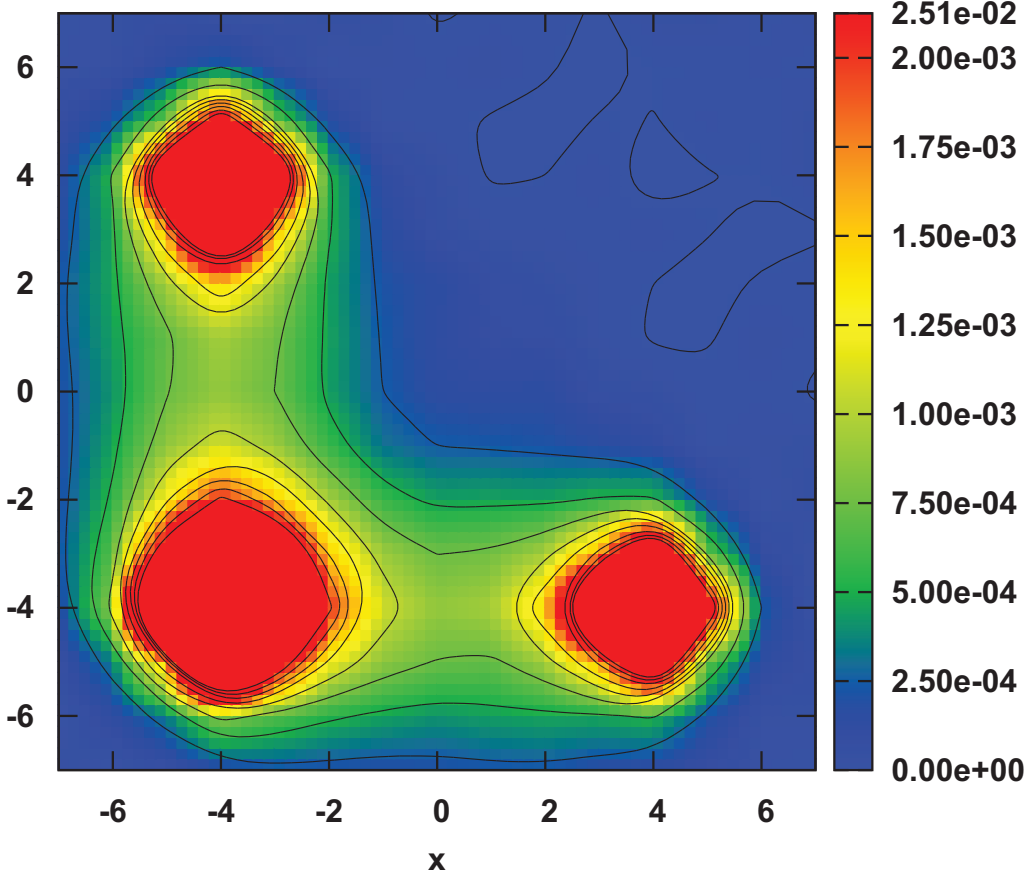
Figure 3: The fields generated by static hybrid sources, notice how the flux organizes into fundamental colour triplet flux tubes.

transformations. In Fig. 6 we extract the string tensions $\sigma(T)$ from the free energy $F_1(T)$ computed by the Bielefeld group, and we also include string tensions previously computed by the Bielefeld group [9].

We also find an ansatz for the string tension curve, among the order parameter curves of other physical systems related to confinement, i. e. in ferromagnetic materials, in the Ising model, in superconductors either in the BCS model or in the Ginzburg-Landau model, or in string models, to suggest ansatze for the string tension curve. We find that the order parameter curve that best fits our string tension curve is the spontaneous magnetization of a ferromagnet [10], solution of the algebraic equation,

$$\frac{M}{M_{sat}} = \tanh\left(\frac{T_c}{T}\frac{M}{M_{sat}}\right) . \tag{2.3}$$

In Fig. 7 we show the solution of Eq. 2.3 obtained with the fixed point expansion, and compare it with the string tensions computed from lattice QCD data.

3. The mass gap equation with finite T and finite current quark mass m_0.

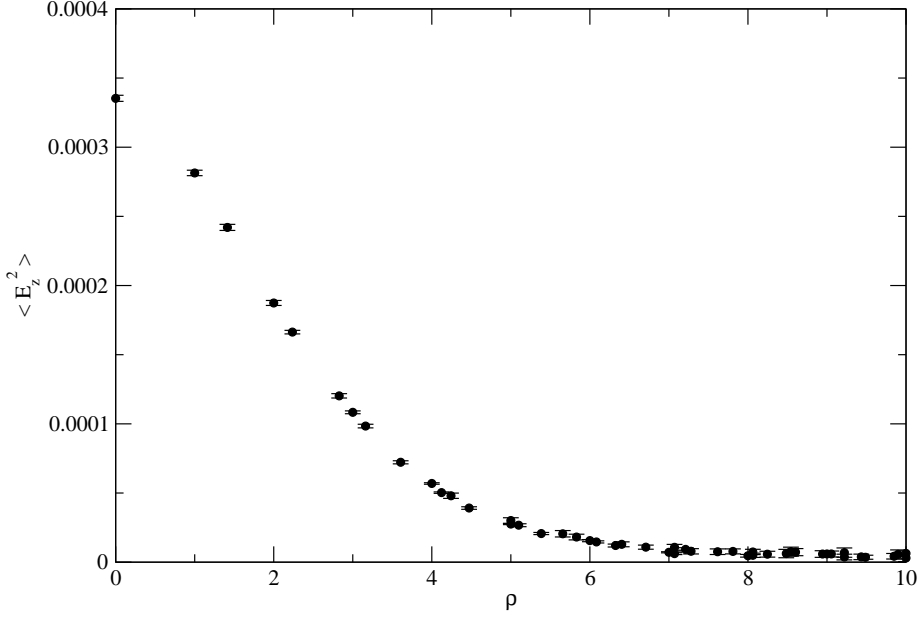Now, the critical point occurs when the phase transition changes to a crossover, and the

Figure 4: The perpendicular profile of the longitudinal electric field, in units of the lattice spacing $a = 0.07261(85) fm$. The flux tube is so thin, that in quark models it is usually modelled by a single parameter, the string tension σ.

crossover in QCD is produced by the finite current quark mass m0, since it affects the order parameters P or σ, and the mass gap $m(0)$ or the quark condensate $\langle \bar{q}q \rangle$. Moreover, using as order parameter the mass gap, i. e. the quark mass at vanishing moment a finite quark mass transforms the chiral symmetry breaking from a phase transition into a crossover. For the study of the QCD phase diagram it thus is relevant to determine how the current quark mass affects chiral symmetry breaking, in particular we study in detail the effect of the finite current quark mass on chiral symmetry breaking, in the framework of truncated Coulomb gauge QCD with a linear confining quark-antiquark potential. In the chiral limit of massless current quarks, the breaking of chiral symmetry is spontaneous. But for a finite current quark mass, some dynamical symmetry breaking continues to add to the explicit breaking caused by the quark mass. The mass gap equation at the ladder/rainbow truncation of Coulomb Gauge QCD in equal time reads,

$$m(p) = m_0 + \frac{\sigma}{p^3} \int_0^\infty \frac{dk}{2\pi} \frac{I_A(p,k,\mu) m(k) p - I_B(p,k,\mu) m(p) k}{\sqrt{k^2 + m(k)^2}} , \tag{3.1}$$

$$I_A(p,k,\mu) = \left[\frac{pk}{(p-k)^2 + \mu^2} - \frac{pk}{(p+k)^2 + \mu^2} \right] ,$$

$$I_B(p,k,\mu) = \left[\frac{pk}{(p-k)^2 + \mu^2} + \frac{pk}{(p+k)^2 + \mu^2} + \frac{1}{2} \log \frac{(p-k)^2 + \mu^2}{(p+k)^2 + \mu^2} \right] .$$

The mass gap equation (3.1) for the running mass $m(p)$ is a non-linear integral equation with a nasty cancellation of Infrared divergences [11, 12, 13]. We devise a new method with a rational ansatz, and with relaxation [14], to get a maximum precision in the IR where the equation extremely large
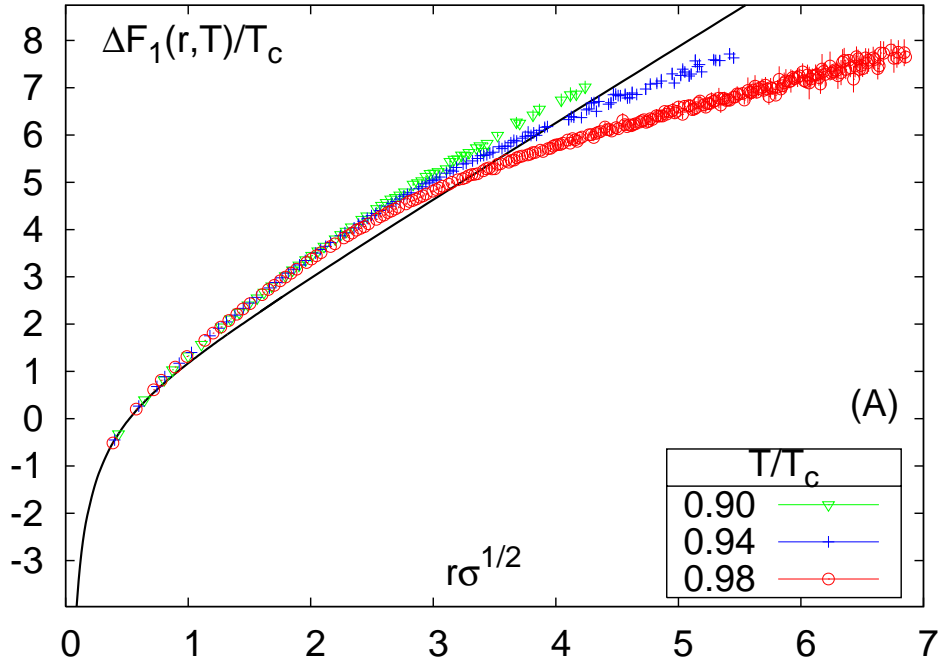
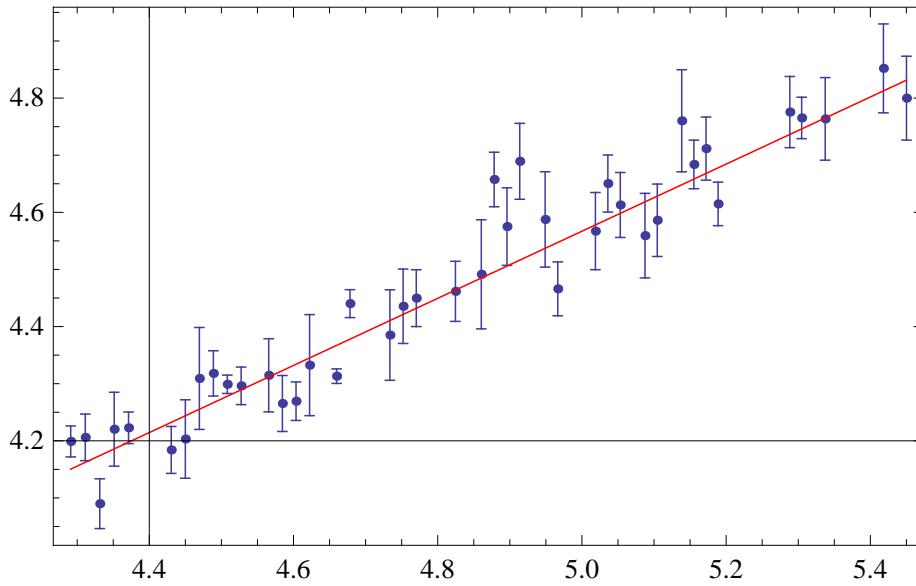**Figure 5:** The Bielefeld free F_1 energy at $T < T_c$.

Figure 6: Detail of the string tension fit in the case of $T = 0.94T_c$. We cut the low distance part in such a way that a linear fit is stable for cuttof changes.

cancellations occur. Since the current quark masses of the six standard flavours u, d, s, c, b, t span over five orders of magnitude from 1.5 MeV to 171 GeV, we develop an accurate numerical method
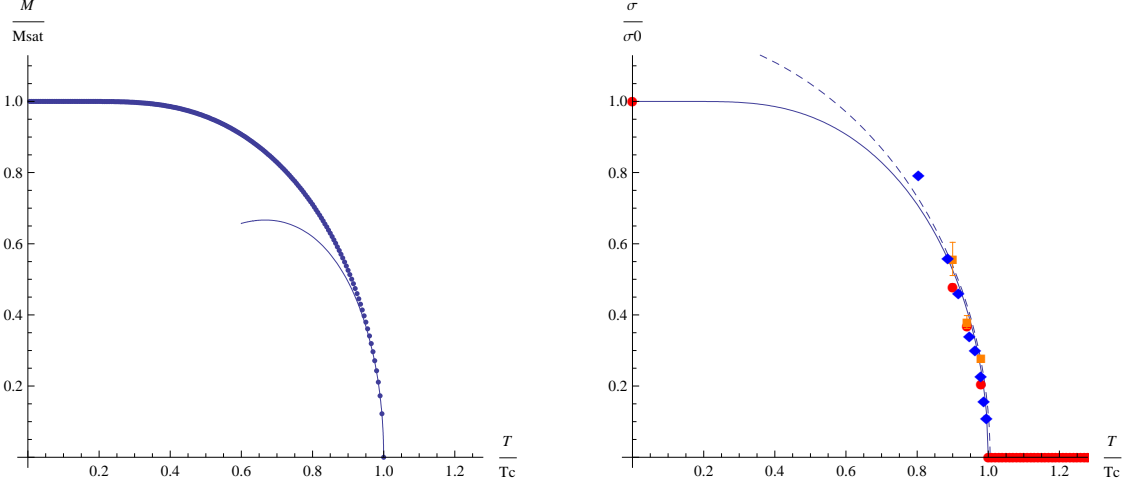
Figure 7: (left) The critical curve for $\frac{M}{M_{sat}}$ as a function of $\frac{T}{T_c}$, for $T \simeq T_c$ it behaves like a square root. (right) comparing the magnetization critical curve with the string tension σ/σ_0, fitted from the long distance part of F_1, they are quite close.

to study the running quark mass gap and the quark vacuum energy density from very small to very large current quark masses. The solution $m(p)$ is shown in Fig. 8 for a vanishing momentum $p = 0$.

At finite T, one only has to change the string tension to the finite T string tension $\sigma(T)$ [15], and also to replace an integral in ω by a sum in Matsubara Frequencies. Both are equivalent to a reduction in the string tension, $\sigma \rightarrow \sigma^*$ and thus all we have to do is to solve the mass gap equation in units of σ^*. The results are depicted in Fig. 8. Thus at vanishing m_0 we have a chiral symmetry phase transition, and at finite m_0 we have a crossover, that gets weaker and weaker when m_0 increases. This is also sketched in Fig. 8.

4. Chiral symmetry and confinement crossovers with a finite current quark mass

We study whether the two main phase transitions in the QCD phase diagram, confinement and chiral symmetry breaking, have two different two critical points or a coincident one. Confinement drives chiral symmetry breaking, and at small density both transitions are a crossover, and not a first or second order phase transition due to the finite quark mass.

However the quark mass affects differently these two phase transitions in the QCD. In what concerns confinement, the linear confining quark-antiquark potential saturates when the string breaks at the threshold for the creation of a quark-antiquark pair. Thus the free energy $F(0)$ of a single static quark is not infinite, it is the energy of the string saturation. The saturation energy is of the order of the mass of a meson i. e. of $2m_0$. For the Polyakov loop we get,

$$P(0) \simeq Ne^{-2m_0/T} .\tag{4.1}$$

Thus at infinite m_0 we have a confining phase transition, while at finite m_0 we have a crossover, that gets weaker and weaker when m_0 decreases. This is sketched in Fig. 9.

Since the finite current quark mass affects in opposite ways the crossover for confinement and the one for chiral symmetry, we conjecture that at finite T and μ there are not only one but two
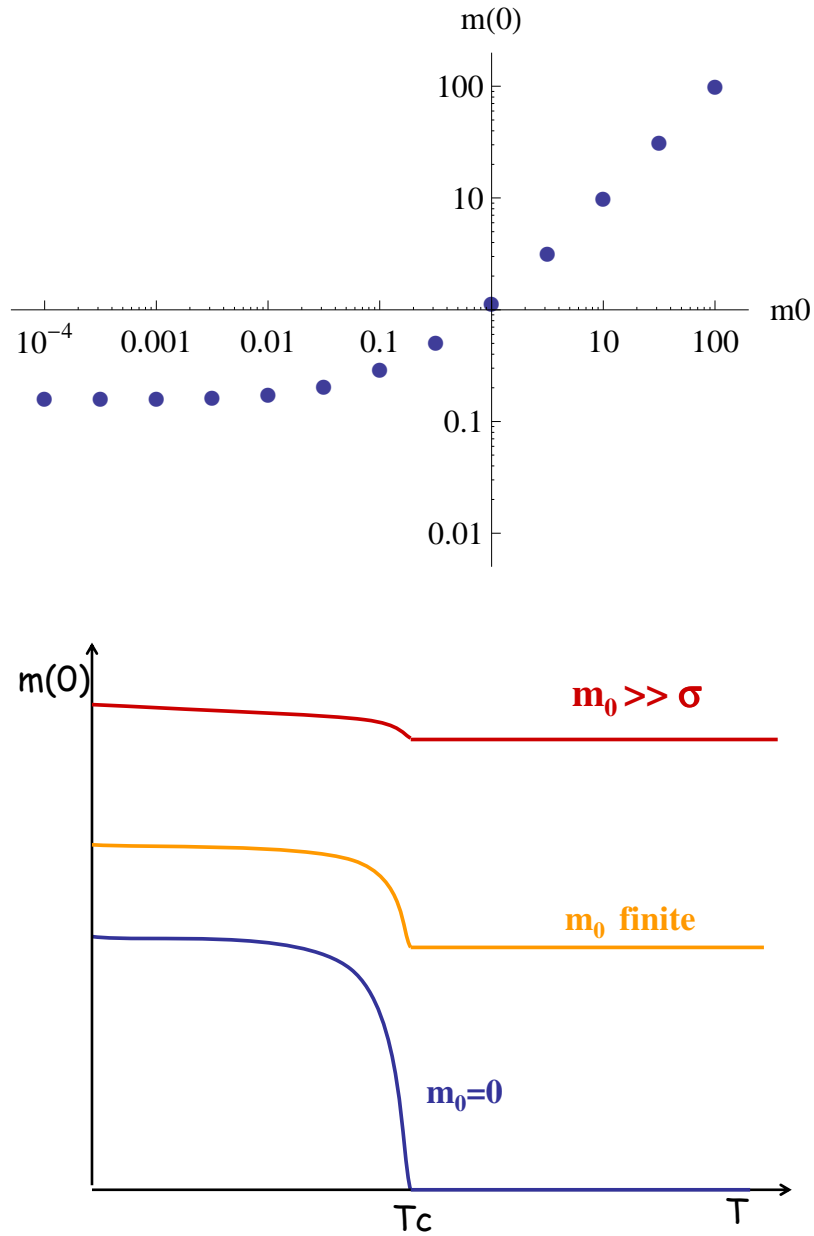
7

Figure 8: (top) The mass gap $m(0)$ solution of as a function of the quark current mass m_0, in units of $\sigma = 1$. (bottom) Sketch of the effect of m_0 on the crossover versus phase transition of chiral restoration at finite T.

critical points (a point where a crossover separates from a phase transition). Since for the light u and d quarks the current mass m_0 is small, we expect the crossover for chiral symmetry restoration critical to be closer to the $\mu = 0$ vertical axis, and the crossover for deconfinement to go deeper into the finite μ region of the critical curve in the QCD phase diagram depicted in Fig. 1.
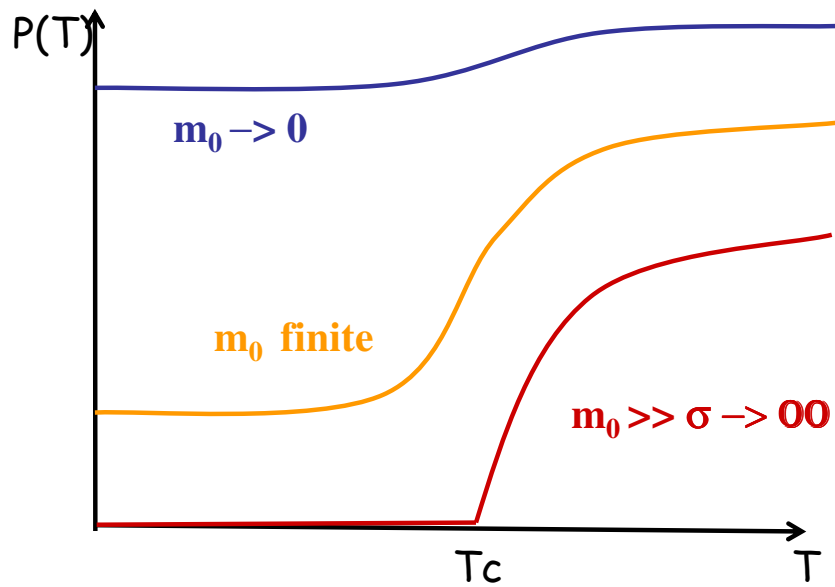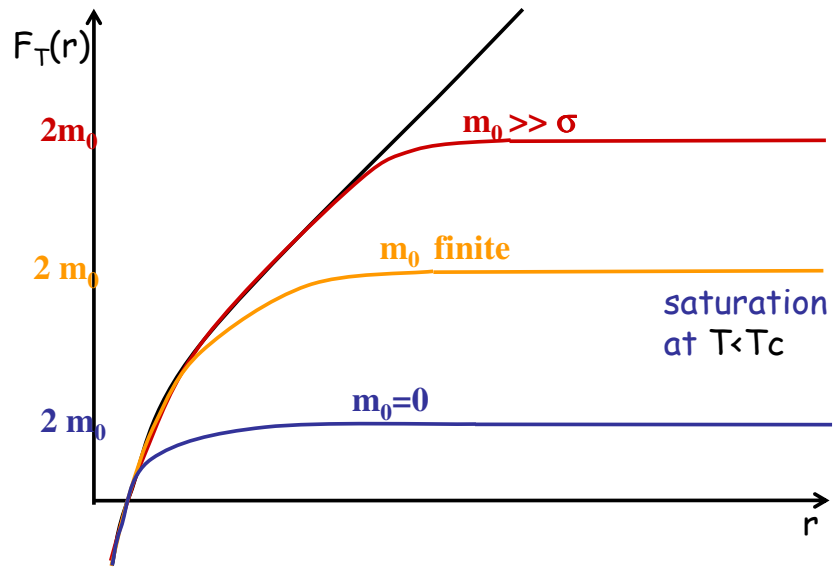
Figure 9: Sketches of the saturation of confinement (top), and of the corresponding crossover in the order parameter P polyakov loop (bottom).

5. Outlook

We soon plan to complete the part of this work which is only sketched here, i. e. to compute

the crossover curves for the chiral symmetry restoration and for the deconfinement at finite T. This will also require the study of light hadrons at finite temperature T. Thus we also plan to address the excited hadron spectrum at finite T, continuing the work initiated with Tim Van Cauteren, Marco Cardoso, Nuno Cardoso and Felipe Llanes-Estrada [2].

References

[1] CBM Progress Report, publicly available at http://www.gsi.de/fair/experiments/CBM, (2009).

[2] P. Bicudo, M. Cardoso, T. Van Cauteren and F. J. Llanes-Estrada, Phys. Rev. Lett. **103**, 092003 (2009) [arXiv:0902.3613 [hep-ph]].

[3] P. Bicudo, Phys. Rev. D **81**, 014011 (2010) [arXiv:0904.0030 [hep-ph]].

[4] M. Doring, K. Hubner, O. Kaczmarek and F. Karsch, Phys. Rev. D **75**, 054504 (2007) [arXiv:hep-lat/0702009].

[5] K. Hubner, F. Karsch, O. Kaczmarek and O. Vogt, arXiv:0710.5147 [hep-lat].

[6] O. Kaczmarek and F. Zantow, Phys. Rev. D **71**, 114510 (2005) [arXiv:hep-lat/0503017].

[7] O. Kaczmarek and F. Zantow, arXiv:hep-lat/0506019.

[8] O. Kaczmarek and F. Zantow, PoS **LAT2005**, 192 (2006) [arXiv:hep-lat/0510094].

[9] O. Kaczmarek, F. Karsch, E. Laermann and M. Lutgemeier, Phys. Rev. D **62**, 034021 (2000) [arXiv:hep-lat/9908010].

[10] R. Feynamn, R. Leighton, M. Sands, "The Feynman Lectures on Physics", Vol II, chap. 36 "Ferromagnetism", published by Addison Wesley Publishing Company, Reading, Massachussets, ISBN 0-201-02117-x (1964).

[11] S. L. Adler and A. C. Davis, Nucl. Phys. B **244**, 469 (1984).

[12] P. J. A. Bicudo and A. V. Nefediev, Phys. Rev. D **68**, 065021 (2003) [arXiv:hep-ph/0307302].

[13] F. J. Llanes-Estrada and S. R. Cotanch, Phys. Rev. Lett. **84**, 1102 (2000) [arXiv:hep-ph/9906359].

[14] P. Bicudo, arXiv:1007.2044 [hep-ph].

[15] P. Bicudo, arXiv:1003.0936 [hep-lat].